SUPPLEMENTARY MATERIAL

Jersin et al. Role of the neutral amino acid transporter SLC7A10 in adipocyte lipid storage, obesity and insulin resistance.

This file includes:

Supplementary Tables:

Supplementary Figures:

Supplementary References

Supplementary Tables

Supplementary Table 1. Primers used for qPCR.

Gene	Forward primer (5' → 3')	Reverse primer (5' → 3')
SLC7A10 Human	CGCCCTCCCCAGTCC	CCCGAGCCGATGATGTTC
*HPRT** Human	TGACCTTGATTTATTTTGCATACC	CGAGCAAGACGTTCAGTCCT
Slc7a10 Mouse	CTTCTGGATGACACCGTCTG	GATGGCACGAGGTAGGTTCT
*Rps13** Mouse	CAGGTCCGTTTTGTGACTG	AGCATCCTTATCCTTTCTGT

* Reference gene

Supplementary Table 2. Characteristics of donors of liposuction material for human primary adipose stromal cell (hASC) cultures.

Donor no.	Figure no.	Age	BMI
1	3C	53	26.4
2	3C	41	32.4
3	3D, 6B	67	26
4	3F, S7B	32	26.9
5	3F, S7B	52	24.3
6	3F, S7C	52	30
7	3F, 6K	52	26.7
8	4B-C, S2A-D, S5A-B, 6D	53	31.5
9*	4B-C, S2A-D, S5A-B, 6D	36	24.3
10	4B-C, S2A-D, S5A-B, 6D	21	29.4
11	4B-C, S2A-D, S5A-B, 6D	58	28
12	4B-C, S2A-D, S5A-B, 6D	45	28.4
13	4B-C, S2A-D, S5A-B, 6D	45	30
14	5A	32	25.5
15	6A, S6A-B	48	27.7
16	6H	46	24.3
17	6H	32	28.4
18	S6B	68	32.8

* Male.

Supplementary Table 3. Plasmids for overexpression.

Vector name	Description	Manufacturer
pCMV6-Kan/Neo	mSlc7a10 (untagged)	Origene
pCMV6-XL4/XL5/XL6	TrueClone^{TM} Empty vector	Origene

Supplementary Table 4. mRNA expression and correlations for identified candidate genes with differential expression in human adipose tissue (Jersin et al. *Diabetes*)

Cohort:		BPD-Fat (n=12)		ADIPO (n=12)						SibPair (n=88)				
		OM/SC	Post/Pre	OM mRNA			SC mRNA			$WHR = \alpha + \beta_1 SEX + \beta_2 BMI + \beta_3 GENE\ EXPRESSION + \varepsilon$				
Symbol	Probe ID	mRNA ratio		Whole	Adipo	SVF	Whole	Adipo	SVF	Probe ID	SC mRNA	R-square*	p-value	pos or neg
Higher in OM vs. SC fat, up-regulated in SC fat after fat loss														
CIDEA	ILMN_2390318	1.70	1.64	1 094	5 627	312	655	2 522	235	221295_at	155	0.520	0.0002	neg
DFNA5	ILMN_1670145	1.77	1.96	920	835	2 344	385	478	1 552	203695_s_at	28.3	0.450	0.122	ns
FLRT2	ILMN_1769615	1.63	1.90	565	255	1 696	313	407	841	204359_at	36.1	0.460	0.048	pos
GAS1	ILMN_2062701	1.73	2.02	1 155	368	2 685	603	256	1 801	204457_s_at	194	0.478	0.010	pos
GPD1L	ILMN_1694106	1.65	1.77	2 049	4 647	2 421	1 193	1 607	1 974	212510_at	95.2	0.590	2.14x10-7	neg
HOXA5	ILMN_1753613	2.38	2.11	1 418	4 692	4 448	800	2 797	2 819	213844_at	50.2	0.469	0.021	neg
SLC7A10	ILMN_1681087	1.83	1.84	1 603	4 986	312	866	2 225	204	220868_s_at	20.5	0.510	0.001	neg
Higher in OM vs. SC fat, down-regulated in SC fat after fat loss														
ALDH1A2	ILMN_1748538	-1.54	2.48	1 686	464	5 459	505	215	814	207016_s_at	18.0	0.498	0.002	pos
GFPT2	ILMN_1709674	-1.93	1.61	1 153	240	1 225	782	243	1 252	205100_at	12.4	0.443	0.247	ns
PDLIM3	ILMN_2230025	-1.55	1.94	989	487	1 478	513	250	676	209621_s_at	7.9	0.448	0.150	ns
TFPI2	ILMN_2068104	-1.52	1.94	577	221	694	269	178	223	209278_s_at	66.8	0.437	0.542	ns
TMEM158	ILMN_1792455	-1.63	1.67	568	285	964	382	304	445	213338_at	2.8	0.472	0.016	pos
Lower in OM vs. SC fat, up-regulated in SC fat after fat loss														
APOC1	ILMN_1789007	3.21	-1.53	309	259	873	544	536	1 556	204416_x_at	50.0	0.445	0.191	ns
COL6A3	ILMN_2307861	1.67	-1.54	3 342	3 154	15 450	5 519	3 276	23 271	201438_at	569	0.447	0.167	ns
CTHRC1	ILMN_2117508	1.52	-2.01	306	154	378	747	180	1122	225681_at	103	0.465	0.029	pos
CTSG	ILMN_1680424	2.41	-1.64	576	181	2 799	1 135	220	7 428	205653_at	14.4	0.515	0.0003	pos
DCLK1	ILMN_2165354	1.98	-1.56	418	396	1 465	696	471	3 725	229800_at	91.2	0.462	0.041	pos
EMX2	ILMN_2187746	1.63	-1.54	151	175	183	239	443	634	221950_at	12.0	0.489	0.003	pos
FNDC1	ILMN_2163873	3.60	-1.62	205	146	299	322	190	2 152	226930_at	13.6	0.443	0.246	ns
PRRX1	ILMN_1739496	1.76	-2.23	1 112	707	4 367	2 266	1 014	11 052	226695_at	202	0.518	0.0002	pos
SERPINA5	ILMN_1759910	1.52	-3.10	165	163	243	559	202	1925	209443_at	12.6	0.468	0.024	pos

Lower in OM vs. SC fat, down-regulated in SC fat after fat loss														
CCND1	ILMN_1688480	-1.62	-3.23	2 587	4 866	3 457	7 409	18 302	4 661	208712_at	124	0.471	0.017	pos
DARC	ILMN_1723684	-1.65	-1.55	2 191	1 169	2 456	3 381	666	3 742	208335_s_at	70.5	0.467	0.025	pos
EGFL6	ILMN_2057479	-5.68	-6.95	351	355	711	3 039	15 392	1 146	219454_at	428	0.461	0.045	pos
GPR56	ILMN_1697228	-2.11	-1.64	868	968	1 455	1 347	624	1 959	212070_at	74.7	0.436	0.563	ns
IFIT3	ILMN_1664543	-1.55	-1.53	214	281	255	321	235	293	229450_at	91.5	0.462	0.040	pos
INHBB	ILMN_1685714	-1.80	-1.53	754	1 584	675	1 205	2 511	940	205258_at	75.5	0.478	0.010	pos
ITIH5	ILMN_1731862	-1.60	-1.67	379	515	230	623	1 088	327	219064_at	457	0.486	0.005	pos
MSC	ILMN_1741404	-2.32	-1.72	341	599	274	578	968	312	209928_s_at	3.3	0.470	0.018	pos
NOTCH3	ILMN_1658926	-1.51	-2.58	480	909	888	1 408	3 183	2 143	203238_s_at	16.5	0.479	0.009	pos
PEMT	ILMN_1745806	-1.51	-2.30	1 129	3 191	798	2 368	10 395	1 665	207621_s_at	138	0.486	0.004	pos
RND3	ILMN_1759513	-3.83	-1.69	2 143	782	1 147	2 996	1 959	1 887	212724_at	83.4	0.469	0.020	pos
SERPINA3	ILMN_1788874	-1.83	-1.66	367	211	624	602	325	1 007	202376_at	4.8	0.457	0.063	ns
SNCG	ILMN_1653161	-2.01	-1.63	566	1 163	327	975	3 253	396	209877_at	18.2	0.440	0.334	ns
SOX7	ILMN_2134056	-3.14	-1.82	495	208	214	764	174	258	228698_at	93.1	0.467	0.024	neg
TNFRSF4	ILMN_2112256	-1.94	-1.55	348	346	470	518	270	541	214228_x_at	6.0	0.454	0.085	ns
TUBB2A	ILMN_2044813	-2.51	-1.82	590	867	325	1 101	2 276	516	204141_at	588	0.492	0.003	pos
UPP1	ILMN_1746837	-2.18	-1.50	1 264	506	772	1 749	640	1 214	203234_at	12.3	0.492	0.003	pos

Adipo, isolated adipocyte fraction; neg, negative correlation; ns, non-significant; OM, omental adipose tissue; pos, positive correlation; Pre, samples obtained before bariatric surgery; Post, samples obtained one year after bariatric surgery; SC, subcutaneous adipose tissue; SVF, stromal vascular fraction; Whole, whole adipose tissue.

Supplementary Table 5. mRNA co-expression with SLC7A10/ASC-1 mRNA in human adipocytes from the ADIPO cohort (12 lean, 12 obese) (Jersin et al. *Diabetes*)

SYMBOL	Coeff.	SYMBOL	Coeff.	SYMBOL	Coeff.	SYMBOL	Coeff.
SLC7A10	*1*	*continued*		*continued*		*continued*	
UTX	*0.909*	CCNH	*0.766*	PHYH	*0.734*	DNAJA3	*0.715*
BCKDHB	*0.895*	PPP1R16A	*0.766*	RAPGEF4	*0.734*	GSDMB	*0.715*
AK3L1	*0.850*	ACOT1	*0.764*	(undefined)	*0.733*	HIBADH	*0.714*
TMEM22	*0.839*	MLYCD	*0.763*	MED26	*0.733*	CD40	*0.714*
RPL34	*0.836*	TP53I13	*0.763*	HIGD2A	*0.733*	TMEM69	*0.713*
LGALS12	*0.830*	UBTD1	*0.760*	C7orf26	*0.733*	LACTB2	*0.713*
BRP44L	*0.826*	CMTM7	*0.760*	ABCC9	*0.732*	MRPL46	*0.713*
COX7C	*0.822*	CCBL2	*0.758*	LOC731007	*0.731*	SOX6	*0.713*
CHL1	*0.822*	FAM73B	*0.758*	POLS	*0.731*	GSDMB	*0.712*
MCCC1	*0.822*	CKB	*0.757*	PIGP	*0.730*	D2HGDH	*0.710*
DHTKD1	*0.821*	MRPS11	*0.756*	C14orf2	*0.730*	FGFRL1	*0.710*
AGT	*0.820*	MOSC2	*0.755*	DTNA	*0.730*	PPP1R1B	*0.710*
SDHB	*0.818*	PCCA	*0.755*	LETMD1	*0.730*	ZFHX4	*0.710*
ACADM	*0.817*	COX5A	*0.755*	TFAM	*0.729*	RHOT1	*0.708*
NDUFB5	*0.812*	RTCD1	*0.755*	MRPS34	*0.729*	(undefined)	*0.708*
MOSC1	*0.808*	CYC1	*0.755*	(undefined)	*0.729*	NAALAD2	*0.708*
COQ9	*0.808*	FLJ23834	*0.754*	CSNK2A1	*0.728*	TXNDC12	*0.707*
C7orf30	*0.803*	AQP7P2	*0.754*	CICE	*0.728*	FABP5	*0.707*
ATL2	*0.802*	RTN3	*0.753*	DTNA	*0.728*	LOC653145	*0.707*
C6orf66	*0.798*	LOC648605	*0.753*	(undefined)	*0.727*	SNX5	*0.706*
C17orf95	*0.795*	ZFPM1	*0.753*	(undefined)	*0.727*	PCBD1	*0.706*
ELOVL3	*0.795*	(undefined)	*0.752*	MRPL21	*0.725*	TSPAN13	*0.706*
VPS54	*0.789*	MCAT	*0.750*	HAX1	*0.724*	ORMDL3	*0.705*
ALDH1L1	*0.789*	LOC652837	*0.749*	CMC1	*0.723*	CNIH	*0.705*
DDT	*0.789*	CAMK1	*0.749*	LOC653479	*0.723*	CCT7	*0.704*
UBE2W	*0.788*	GART	*0.748*	UCKL1	*0.723*	PATL1	*0.703*
UQCRFS1	*0.788*	XRN1	*0.748*	SLC25A4	*0.722*	ARIH1	*0.703*
BTF3L4	*0.784*	THYN1	*0.747*	LDHD	*0.722*	CLPP	*0.703*
ANO6	*0.784*	COX5B	*0.746*	C12orf45	*0.722*	CASD1	*0.702*
RDH10	*0.783*	PXMP2	*0.746*	DMRT2	*0.721*	C4orf14	*0.702*
UQCRH	*0.783*	POLR1D	*0.745*	PXMP2	*0.720*	AUH	*0.701*
LOC646345	*0.780*	LOC648695	*0.745*	SH3GLB1	*0.720*	BCKDHB	*0.701*
C7orf44	*0.780*	AK3L1	*0.743*	C2orf56	*0.719*	RFXANK	*0.701*
PCK1	*0.776*	FAM18B	*0.743*	FAM152B	*0.718*	SCO1	*0.701*
ATP5F1	*0.776*	SLC2A1	*0.742*	PCGF6	*0.718*	LOC650494	*0.701*
HSPD1	*0.775*	HIST1H2BD	*0.742*	CCNF	*0.718*	LOC643300	*0.700*
KIAA1191	*0.773*	C21orf70	*0.741*	EXOSC3	*0.718*	GOT1	*0.700*
ACAD8	*0.772*	AK2	*0.741*	ALKBH1	*0.718*	SYPL1	*0.700*
ESRRA	*0.771*	CDH23	*0.739*	PCBD1	*0.717*	DCI	*0.699*
ABHD3	*0.771*	CYB5A	*0.738*	BPHL	*0.717*	MCCC2	*0.699*
SLC25A5	*0.770*	C21orf33	*0.738*	SLC25A40	*0.716*	ACOT2	*0.699*
MRPL41	*0.770*	CS	*0.737*	ATP1B3	*0.716*	(undefined)	*0.699*
ELK1	*0.769*	ENDOG	*0.737*	FBXO21	*0.715*	STOX1	*0.698*
TMLHE	*0.767*	BCKDHB	*0.736*	MRPS22	*0.715*	FRMD4A	*0.698*
C2orf47	*0.767*	MRPL33	*0.735*	ZNF280D	*0.715*	WDR43	*0.698*
SYMBOL	**Coeff.**	**SYMBOL**	**Coeff.**	**SYMBOL**	**Coeff.**	**SYMBOL**	**Coeff.**

continued		*continued*		*continued*		*continued*	
RPAIN	*0.698*	CALML4	*0.687*	TMCO6	*0.674*	MACROD1	*0.660*
MTFMT	*0.698*	RDH14	*0.687*	SEC24B	*0.674*	CA2	*0.659*
SLC4A4	*0.698*	TAF1L	*0.686*	(undefined)	*0.674*	GTF2IRD1	*0.659*
DTNA	*0.698*	DDX47	*0.685*	PRIM1	*0.674*	C17orf61	*0.658*
ANKRD11	*0.697*	CDKN2C	*0.685*	LETMD1	*0.673*	FBXO46	*0.658*
QPCT	*0.697*	THYN1	*0.684*	GBE1	*0.673*	HSCB	*0.658*
FGFRL1	*0.696*	SDHA	*0.682*	TYSND1	*0.673*	NDUFV2	*0.658*
MRPL39	*0.696*	SNORD100	*0.682*	EBAG9	*0.672*	LOC643466	*0.657*
VPS26B	*0.696*	SUMO2	*0.682*	MRPS23	*0.671*	NDUFB11	*0.656*
KIAA0261	*0.696*	KLF15	*0.682*	TMLHE	*0.671*	MGC70857	*0.656*
GCHFR	*0.695*	HSD17B10	*0.681*	MESP1	*0.671*	(undefined)	*0.656*
C1orf66	*0.695*	GNAQ	*0.681*	CPEB2	*0.671*	NDUFV3	*0.655*
SPTB	*0.695*	CMTM7	*0.681*	MKNK2	*0.670*	PMPCB	*0.655*
STRADB	*0.695*	RABGGTB	*0.681*	(undefined)	*0.670*	(undefined)	*0.655*
VPRBP	*0.694*	GGCT	*0.681*	ALDH6A1	*0.670*	VPS35	*0.655*
PLAGL2	*0.694*	SLC3A2	*0.681*	FBXO28	*0.669*	LPIN1	*0.655*
SLC16A7	*0.694*	CNBP	*0.680*	C2orf56	*0.669*	AASDHPPT	*0.655*
ACADL	*0.694*	RSBN1	*0.680*	AGPAT2	*0.669*	LOC642335	*0.655*
NDUFB6	*0.694*	RBMS2	*0.680*	PPARG	*0.669*	NPC1	*0.654*
CRLS1	*0.694*	SCP2	*0.680*	PIGP	*0.668*	SLC2A4	*0.654*
BDH1	*0.693*	(undefined)	*0.680*	STK35	*0.668*	RAVER1	*0.654*
SPRYD4	*0.693*	LOC284023	*0.679*	MAD2L1BP	*0.668*	DAP3	*0.654*
ACADM	*0.693*	(undefined)	*0.679*	CMTM7	*0.667*	L2HGDH	*0.653*
ACP1	*0.693*	ALKBH1	*0.679*	INTS6	*0.667*	MAZ	*0.653*
NCOR2	*0.693*	ZNF280D	*0.679*	SOSTDC1	*0.666*	FMO5	*0.653*
COX6A1	*0.693*	SCN3A	*0.678*	LIX1L	*0.665*	EIF3M	*0.653*
MRPS2	*0.692*	C17orf95	*0.678*	PIK3CB	*0.665*	SEC11A	*0.653*
C9orf72	*0.692*	(undefined)	*0.678*	CS	*0.664*	(undefined)	*0.653*
GFPT1	*0.692*	CNIH	*0.678*	AQP7	*0.664*	PCNX	*0.652*
MLX	*0.692*	CA2	*0.678*	ANKRD9	*0.664*	YPEL5	*0.652*
SNURF	*0.692*	SEPHS1	*0.678*	PDZD7	*0.664*	NDFIP2	*0.652*
BLOC1S1	*0.691*	ESRRAP2	*0.677*	ATAD2	*0.663*	NAT5	*0.652*
PAXIP1	*0.691*	LOC729317	*0.677*	SFXN2	*0.663*	(undefined)	*0.652*
UTP18	*0.691*	(undefined)	*0.677*	MEIS2	*0.663*	HYLS1	*0.652*
C18orf8	*0.690*	NET1	*0.677*	GTPBP3	*0.663*	RPL35A	*0.652*
GLRX2	*0.690*	MCM7	*0.677*	RAB40C	*0.663*	STOX1	*0.651*
LOC652545	*0.690*	DUSP4	*0.677*	TBP	*0.663*	STAMBP	*0.651*
GRPEL1	*0.690*	ICAM3	*0.676*	CLK2	*0.663*	DHPS	*0.651*
CCNC	*0.689*	DNAH1	*0.676*	SEC24B	*0.662*	STBD1	*0.650*
TRPT1	*0.689*	CSNK2A2	*0.676*	NDUFAF2	*0.662*	FBXO44	*0.650*
PATZ1	*0.689*	LOC285074	*0.676*	HINT3	*0.662*	OXA1L	*0.650*
SLC25A22	*0.689*	C16orf14	*0.676*	LOC645436	*0.662*	(undefined)	*0.650*
PC	*0.689*	RPL9	*0.675*	PPP2R2D	*0.662*	ACY1	*0.650*
SMARCD1	*0.688*	(undefined)	*0.675*	(undefined)	*0.661*		
UBQLN1	*0.688*	KIAA0367	*0.675*	PLCXD1	*0.660*		
CASZ1	*0.688*	C1QL2	*0.675*	TCF12	*0.660*		
LDLRAD1	*0.688*	PCCB	*0.675*	ZNF512B	*0.660*		
CXorf15	*0.687*	POLE	*0.674*	MIA3	*0.660*		
	Coeff.	**SYMBOL**	**Coeff.**	**SYMBOL**	**Coeff.**	**SYMBOL**	**Coeff.**

SYMBOL							
(undefined)	*-0.650*	*continued*		*continued*		*continued*	
IFT57	*-0.651*	CANX	*-0.676*	SETBP1	*-0.703*	TLN1	*-0.769*
OLFML1	*-0.651*	ITGA11	*-0.676*	DAB2	*-0.704*	CCNYL1	*-0.769*
TFPI	*-0.652*	CPD	*-0.677*	ZYX	*-0.705*	RAP2A	*-0.771*
C5orf5	*-0.652*	LAPTM5	*-0.677*	SOX4	*-0.705*	FBLN2	*-0.775*
ST5	*-0.653*	ANXA11	*-0.677*	EMX2	*-0.705*	RUFY3	*-0.781*
COL6A2	*-0.653*	FAM129A	*-0.677*	C21orf51	*-0.705*	TMSB10	*-0.786*
CCDC25	*-0.654*	AP1S2	*-0.677*	ACTG1	*-0.707*	IQSEC2	*-0.787*
HABP4	*-0.655*	THBS2	*-0.678*	ZNF219	*-0.709*	PTTG2	*-0.793*
CILP	*-0.655*	ARHGAP28	*-0.678*	COL4A5	*-0.711*	MGP	*-0.845*
LOC648470	*-0.655*	FBLN5	*-0.678*	PDLIM7	*-0.711*	RANBP3L	*-0.846*
PDCL3	*-0.657*	SLC7A2	*-0.679*	RNASEL	*-0.711*		
(undefined)	*-0.657*	MYO1B	*-0.680*	MAP1B	*-0.713*		
KIAA1160	*-0.657*	C1orf24	*-0.681*	STX2	*-0.714*		
KCTD12	*-0.658*	MTTP	*-0.681*	PSAP	*-0.716*		
LOC651302	*-0.659*	SPARC	*-0.681*	ANKS1B	*-0.717*		
TMEM119	*-0.659*	CALM3	*-0.684*	DKK3	*-0.719*		
LUM	*-0.660*	CDH11	*-0.684*	RCN1	*-0.720*		
ITIH5	*-0.661*	ACTB	*-0.685*	SPON2	*-0.723*		
TRPV2	*-0.661*	CAPZB	*-0.685*	DGKI	*-0.724*		
LOC390956	*-0.661*	(undefined)	*-0.685*	CAPNS1	*-0.726*		
CLN5	*-0.662*	LOC389958	*-0.686*	SLC2A12	*-0.726*		
ACTN4	*-0.662*	REEP5	*-0.688*	SAP18	*-0.727*		
(undefined)	*-0.663*	CCDC105	*-0.688*	RNASEL	*-0.732*		
LMOD1	*-0.663*	ACTB	*-0.689*	LOX	*-0.735*		
IFITM5	*-0.663*	DAAM2	*-0.689*	MYO1D	*-0.738*		
(undefined)	*-0.663*	SLC39A3	*-0.689*	SH3BGRL2	*-0.741*		
(undefined)	*-0.664*	CCBP2	*-0.690*	CDC26	*-0.741*		
FLJ22374	*-0.665*	ARHGAP21	*-0.691*	MED20	*-0.742*		
BICD2	*-0.666*	VWA1	*-0.693*	KIAA1598	*-0.742*		
NEXN	*-0.666*	COL4A5	*-0.694*	TAX1BP3	*-0.743*		
CLEC3B	*-0.668*	LPAR1	*-0.694*	DPT	*-0.748*		
(undefined)	*-0.668*	CNN3	*-0.696*	TMEM98	*-0.748*		
SRI	*-0.669*	INHBB	*-0.698*	MGP	*-0.749*		
PON2	*-0.669*	DCTN1	*-0.699*	EMX2	*-0.751*		
CYLN2	*-0.671*	CXCL12	*-0.700*	ABHD4	*-0.754*		
CETN2	*-0.673*	CCND2	*-0.701*	DRAM	*-0.756*		
LOC391013	*-0.673*	PFKP	*-0.701*	ITGA11	*-0.757*		
CANX	*-0.675*	CAMK1D	*-0.702*	(undefined)	*-0.766*		
ITGB5	*-0.675*	ASCC3	*-0.702*	ITGB1	*-0.768*		

Coeff., Pearson's correlation coefficient; SYMBOL, Gene name.

Supplementary Figures

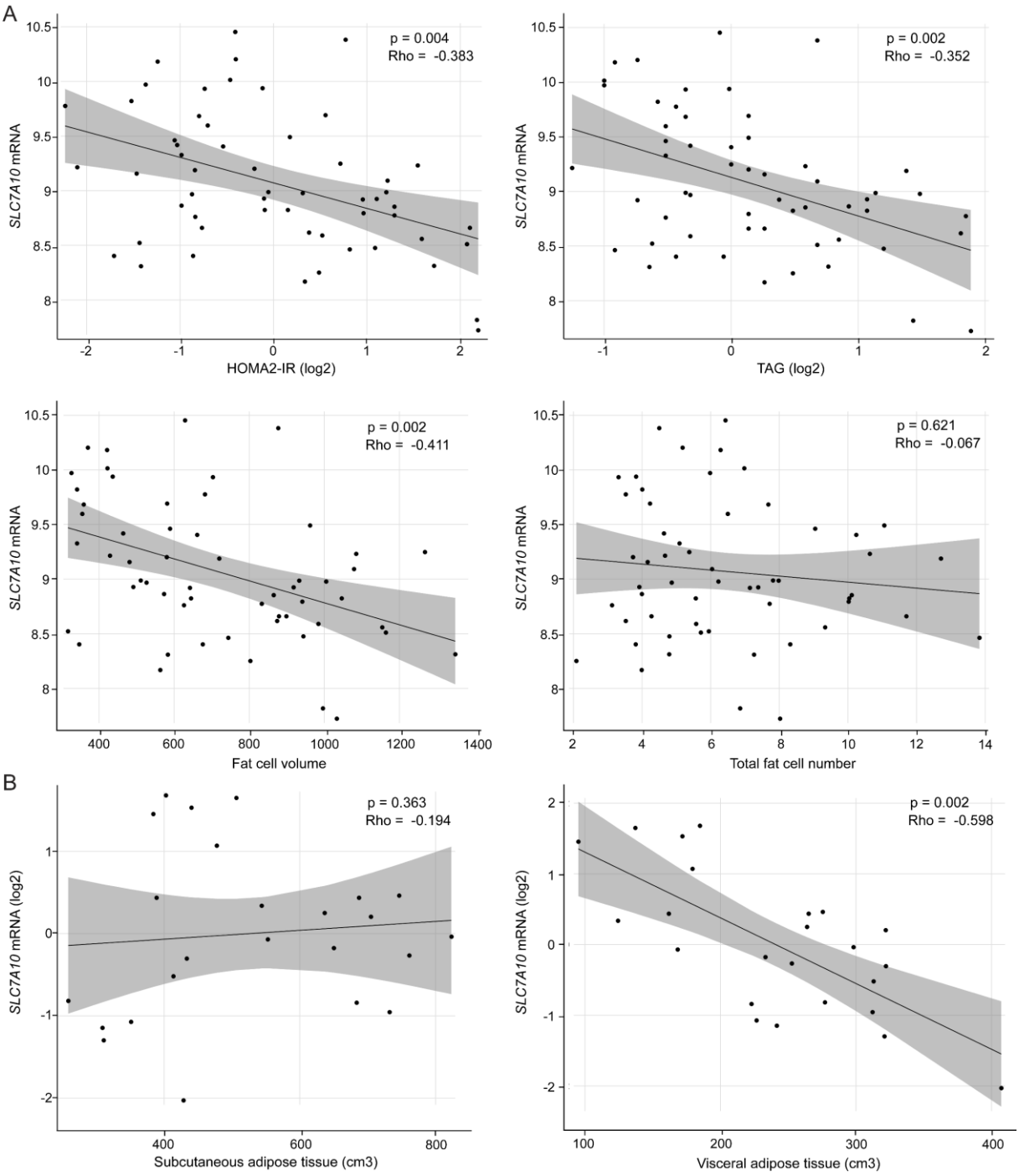

Supplementary Figure 1. Correlations of *SLC7A10* mRNA expression with insulin resistance and adiposity traits in the RIKEN (n=58, panel A) and Sib Pair-Subgroup (n=24, panel B) cohorts.
SLC7A10 mRNA expression was retrieved from microarray expression analyses (Affymetrix) and Spearman correlations were calculated.

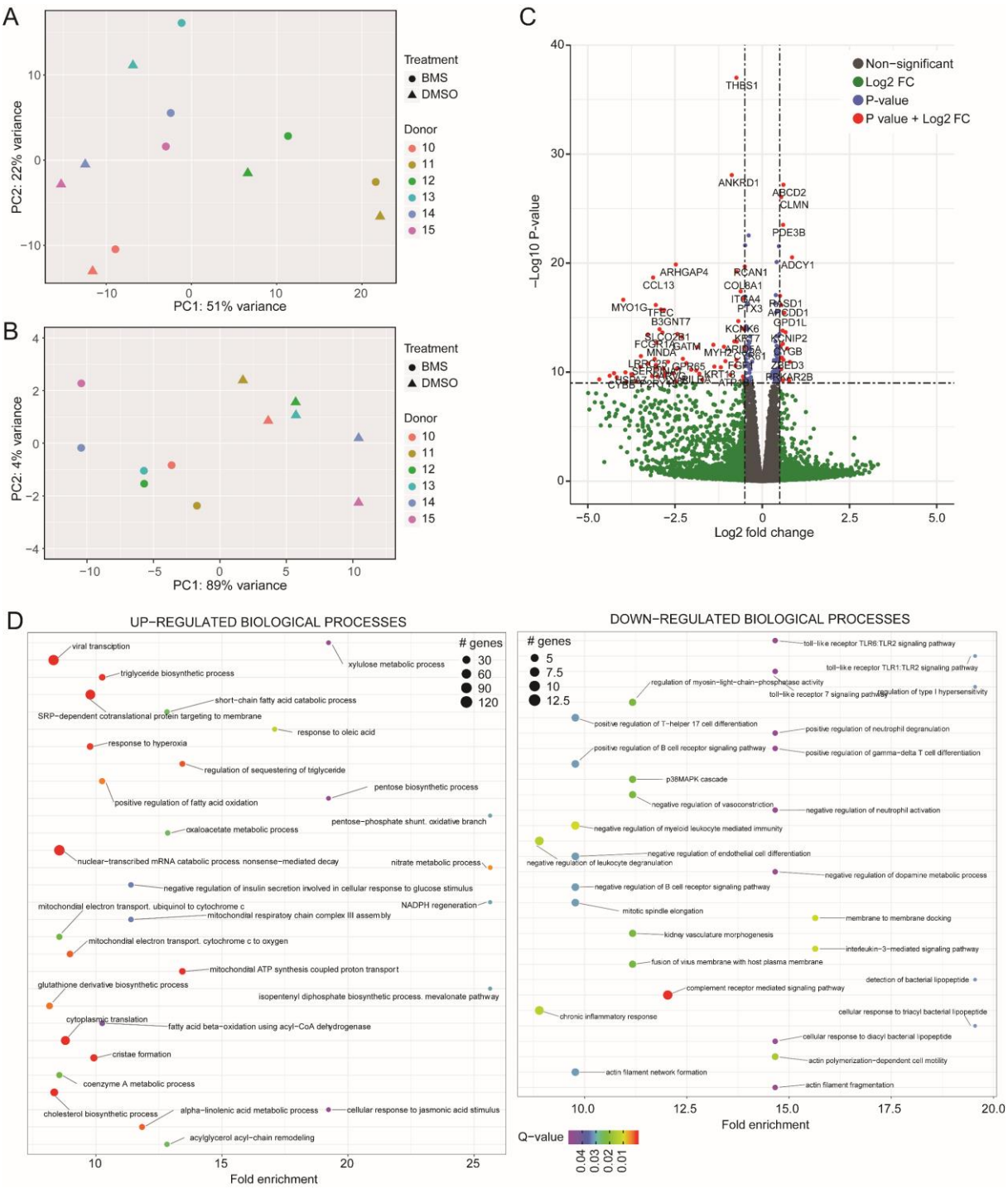

Supplementary Figure 2. Effects of SLC7A10 inhibition on global gene expression measured by RNA-sequencing in human primary adipocytes.

Human adipose stromal cell (hASC) cultures were obtained from abdominal subcutaneous adipose tissue (n=6), differentiated for 8 days, and treated with DMSO or SLC7A10 inhibitor 1 for 24 hours from day 7-8. Global gene expression was measured by RNA-seq, where sample reads were mapped against the Human genome (GrCH38) using HiSat (Version 2.1.0), with options –t "exon" and –g "gene_id" to summarize count values from individual exons into genes, resulting in a matrix of raw counts. Aligned reads were then put into featureCounts (Version 1.5.2) with default options, resulting in a matrix of raw counts. Data were normalized and differential expression analysis was performed utilizing DESeq2 (Version 1.22.2). Pathway analysis of RNA sequencing data was performed using PANTHER classification system (PANTHER v.14.0). Differentially expressed genes identified with a FDR cut-off ($p<0.05$) were used as input and Fischer's exact test was used to identify statistically over/under represented pathways with a FDR cut-off ($p<0.05$) (1). Significant ontologies were visualized using ggplot2 package (Version 3.1.0).

(**A-B**) Principal component (PC) analysis of samples in DMSO and SLC7A10 inhibitor 1 treated groups are shown in (A) unadjusted and (B) adjusted for patient.

(**C**) Volcano plot of differentially expressed genes between DMSO and SLC7A10 inhibitor 1 treatments. x-axis corresponds to log2 fold change (log2FC) and y-axis corresponds to -log10 (P-value). Red dots represent the transcripts with an absolute log2FC > 0.5 and P-value < 10E-10; green dots represent the transcripts with an absolute log2FC > 0.5; blue dots represent transcripts with P-value < 10E-10; grey dots represent transcripts which do not pass above thresholds.

(**D**) Enrichment plot representing up-regulated and down-regulated biological processes between DMSO and SLC7A10 inhibitor treatments. Top 30 biological processes with an FDR-corrected P-value < 0.05 and fold enrichment ≥ 8 (arbitrary threshold for the sake of visual representation) are reported here. Gene Ontology (GO) terms was analyzed by PANTHER (www.pantherdb.org).

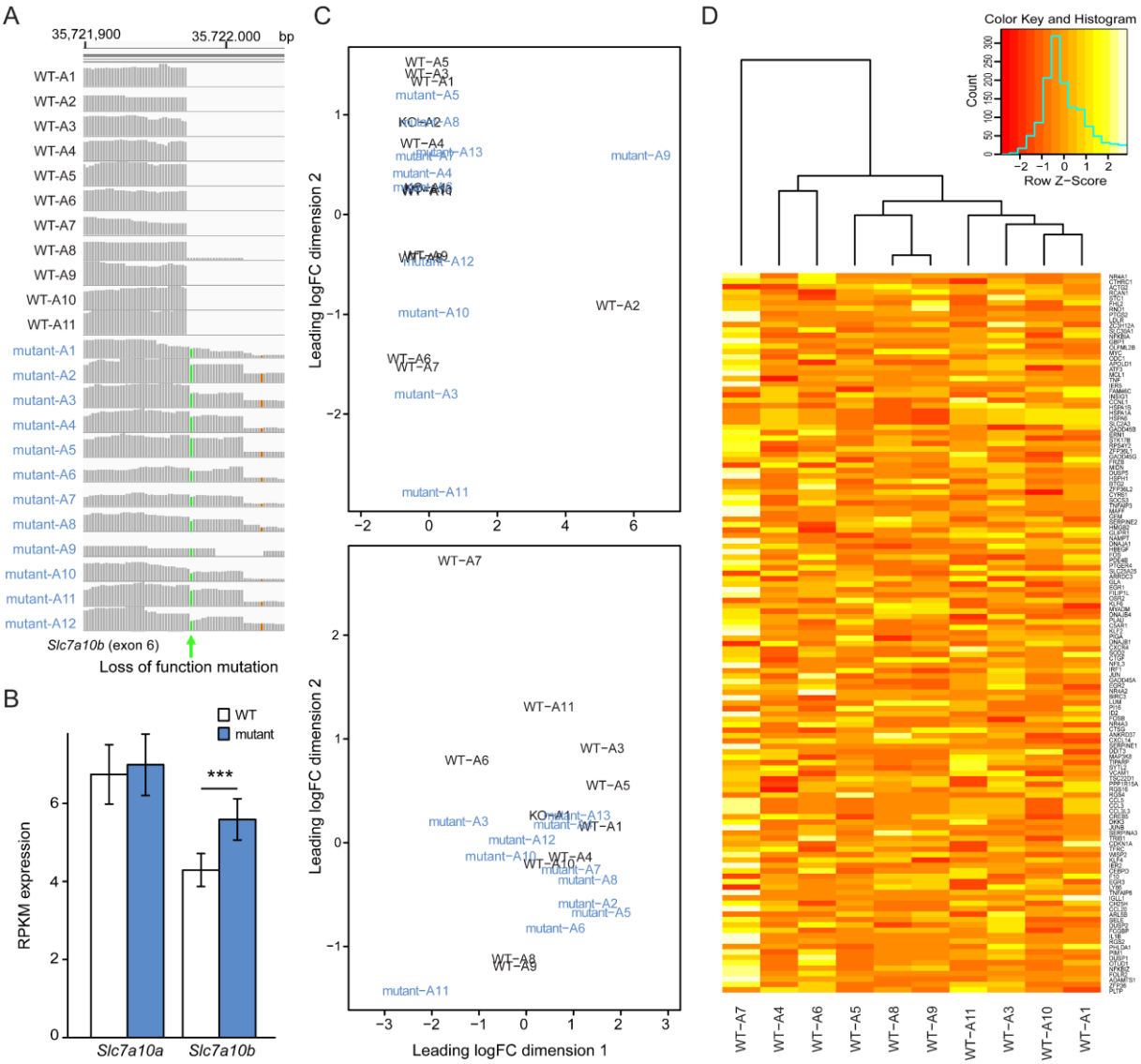

Supplementary Figure 3. Confirmation of Slc7a10b loss-of-function mutation and outlier detection by RNA-sequencing of zebrafish visceral adipose tissue.
Mature (four-month old) wildtype (WT) and Slc7a10b mutant male zebrafish were fed 50-100% more than their regular feed for eight weeks. Visceral adipose tissue from three zebrafish housed in the same tank during the overfeeding was pooled. RNA was isolated and RNA-seq was performed. Sample reads were mapped against the

Zebrafish genome (GRCz10) using HiSat (Version 2.05), matrixed in featureCounts (Version 1.5.2) and analyzed using DESeq2 (version 1.22.1).

(**A**) Integrative genomics viewer (IGV) read visualization of each Zebrafish sample at the target site, with the A→T splice site mutation sa15382 highlighted in green.

(**B**) Visualized expression values (RPKM) of average *Slc7a10a* and *Slc7a10b* expression in both WTs and mutants.

(**C**) Outlier removal of anomalous RNA-Seq sequence reads (by sample) was performed by generating multidimensional scaling plots of distances between digital gene expression profiles. The samples mutant-A9 and WT-A2 were visually identified in the top graph as being erroneous due to their spread from the main cluster in the first dimension. The lower graph displays the distances after the removal of the first two outliers, showing WT-A7 spreading from the main cluster.

(**D**) The differential expression in WT-A7 was further investigated by utilizing the ontology gene expression profiles of the WT samples, and we observed that this sample differed significantly from other wild-types in the expression profile of stress-induced genes identified in human adipose tissue, warranting removal of WT-A7 from further downstream analysis. The stress-induced genes were identified by microarray analysis of omental human adipose tissue biopsies of non-obese patients. Omental biopsies from four patients were either frozen immediately or ~1 hour after surgical excision. The 1-hour delayed freezing induced a large array of immediate-early stress-responsive genes including IL8 (induced already after 10 minutes) [24], largely recapitulating differences we previously observed between lean and extremely obese patients [153] (data not shown). We concluded that the WT-A7 sample was acutely stressed either *in vivo* or *ex vivo*, and that its inclusion in our initial analysis was entirely responsible for an apparent down-regulation of stress-responsive/inflammatory genes in the mutant compared to WT zebrafish. WT-A7 was therefore removed from further analysis, to avoid a dominating artefactual impact on gene ontology terms.

***, $p<0.001$.

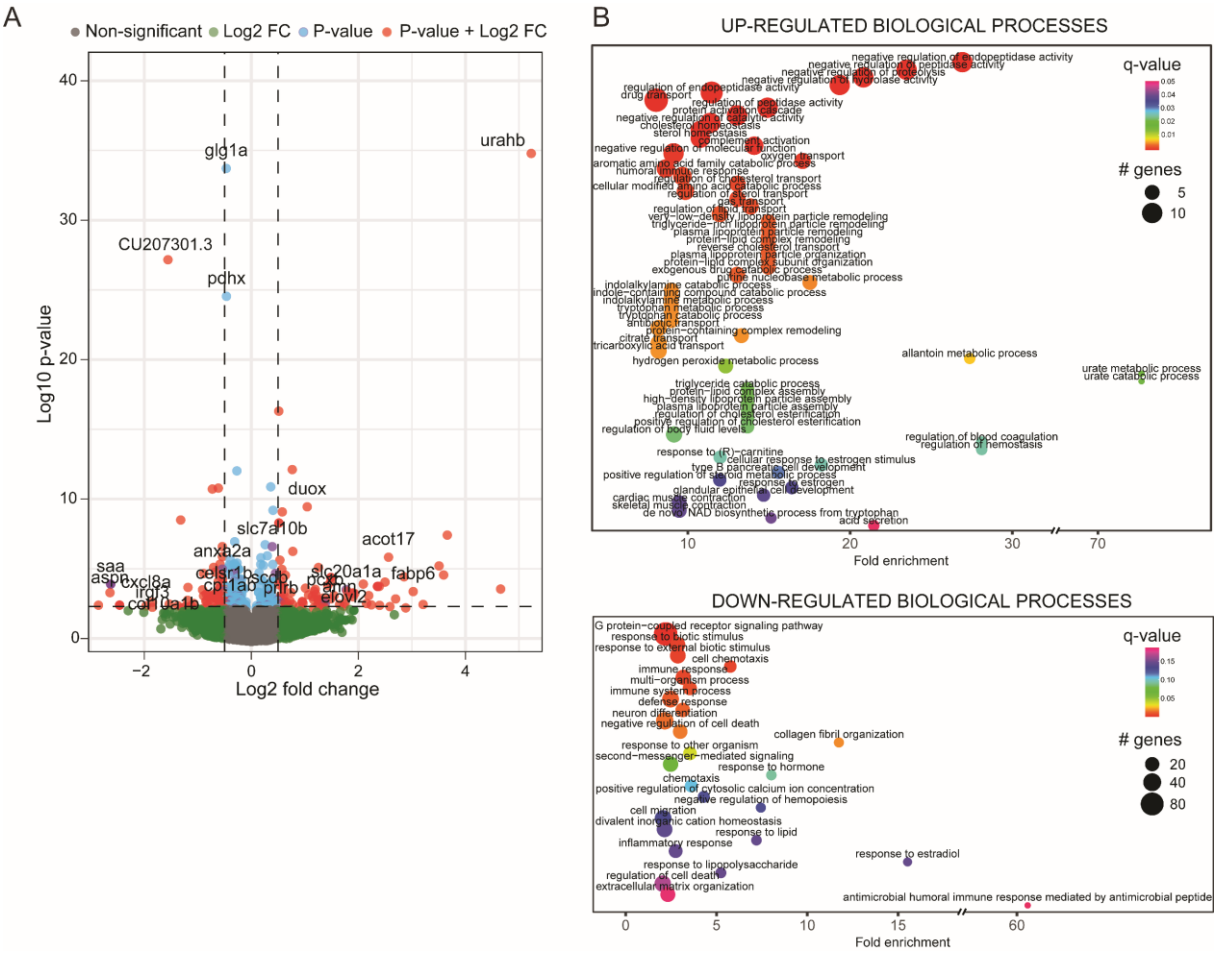

Supplementary Figure 4. Slc7A10b loss-of-function mutation in overfed zebrafish upregulates genes involved in urate, purine, and lipid metabolic processes.
Mature (four-month old) wildtype (WT) and Slc7a10b loss-of-function male zebrafish were fed 50-100% more than their regular feed for eight weeks. Visceral adipose tissue from three zebrafish housed in the same tank during the overfeeding was pooled. RNA was isolated and RNA-seq was performed. Sample reads were mapped against the Zebrafish genome (GRCz10) using HiSat (Version 2.05), matrixed in featureCounts (Version 1.5.2) and analyzed using DESeq2 (version 1.22.1).

(A) Volcano plot of differentially expressed genes between WT and Slc7a10b loss-of-function zebrafish. x-axis corresponds to log2 fold change (log2FC) and y-axis corresponds to -log10 (P-value). The red dots represent the transcripts with an absolute log2FC > 0.5 and P-value < 10E-10; green dots represent the transcripts with an absolute log2FC > 0.5; blue dots represent transcripts with P-value < 10E-10; grey dots represent transcripts which do not pass above thresholds.

(B) Combined differentially expressed genes between Slc7a10b zebrafish WT and mutant into a single ranked list based on fold change, and gene ontology (GO) terms were analyzed using GOrilla (2). Enrichment plot representing up-regulated biological processes between WT and Slc7a10b loss-of-function zebrafish was visualized using the R package ggplot2. Biological processes with a P-value < 0.05 and fold enrichment ≥ 8 (arbitrary threshold for the sake of visual representation) are reported here.

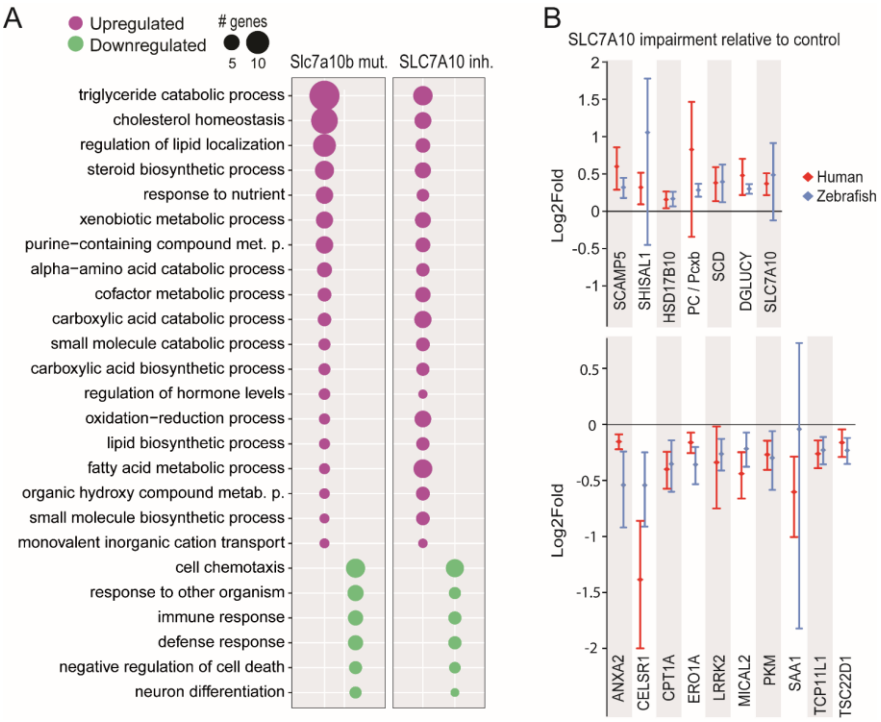

Supplementary Figure 5. SLC7A10 impairment affects genes related to lipid- and energy metabolism in zebrafish adipose tissue and human primary adipocyte cultures.
RNA-sequencing was performed as described in Supplementary Figures 2 and 4. For each dataset, genes were sorted based on fold change into a single ranked list, and analyzed using GOrilla to identify enriched ontologies (2). Significant ontologies were summarized for plotting utilizing the REViGO web package, which clusters representative ontologies via semantic similarity (3). RPKM values for gene expression visualizations were generated using edgeR (Version 3.16.5). Overlapping ontologies between zebrafish adipose tissue and human adipose cultures were plotted using ggplot2 (Version 3.1.0).

(**A**) Gene ontologies enriched with differentially expressed genes identified in RNA-seq from both zebrafish mutant and SLC7A10 inhibitor treated human adipocytes compared to control. Differentially expressed genes were combined into a single ranked list based on fold change using GOrilla analysis (2). Enriched ontologies in both the zebrafish mutant and SLC7A10 inhibitor 1 RNA-seq were aggregated, filtered by enrichment and significance, and plotted by relative enrichment. Overlapping ontologies between Zebrafish and SLC7A10 inhibitor 1 RNA-seq were visualized using the R package ggplot2 (Version 3.1.0).

(**B**) Fold changes for up- and down-regulated genes in RNA-seq from both zebrafish mutant and SLC7A10 inhibitor 1 treated (10 µM) human adipocytes compared to control. Outliers were removed using Whiskers Tukey outlier test. Data are presented as mean ± SD.

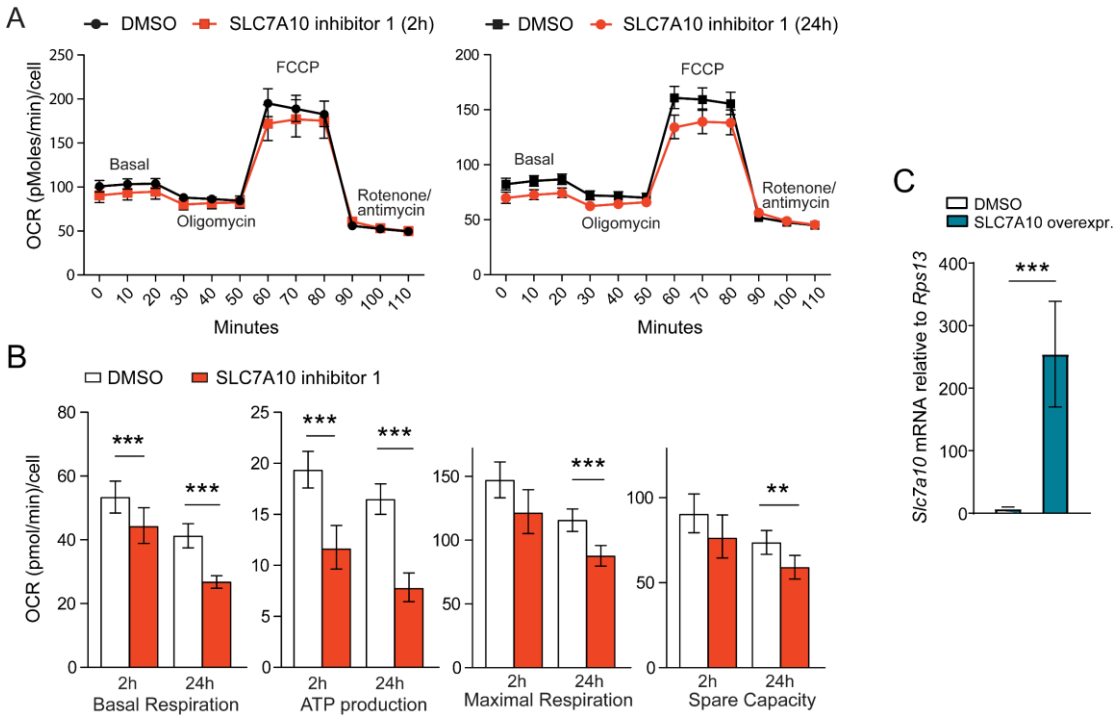

Supplementary Figure 6. SLC7A10 inhibition affects mitochondrial respiration in cultured mouse adipocytes.
3T3-L1s were differentiated and treated with SLC7A10 inhibitor 1 for either 2 or 24 hours, or Slc7a10 was overexpressed every second day from day 2-8.

(A) OCR was measured at day 8 of differentiation under basal conditions and after sequential addition of the following compounds at indicated final concentrations; oligomycin (3 µM); FCCP (1.5 µM); rotenone (1 µM) and antimycin A (1 µM).

(**B**) Outliers were removed based on a Whisker Tukey test of the OCR data for each time point in each well, before calculation of basal respiration, ATP production, maximal respiration and spare respiratory capacity according to the manufacturer's protocol. Results are presented as geometric mean ± 95% confidence interval (n=22-24 replicate wells in a 96-well plate).

(**C**) 3T3-L1 preadipocytes were induced to differentiate and transfected with *Slc7a10* expression plasmid or empty vector on every second day of differentiation (days 2, 4 and 6) and mRNA was collected on day 8. Slc7a10 expression was quantified by qPCR relative to Rsp13 expression (n=3)

**, p<0.01. ***, p<0.001.

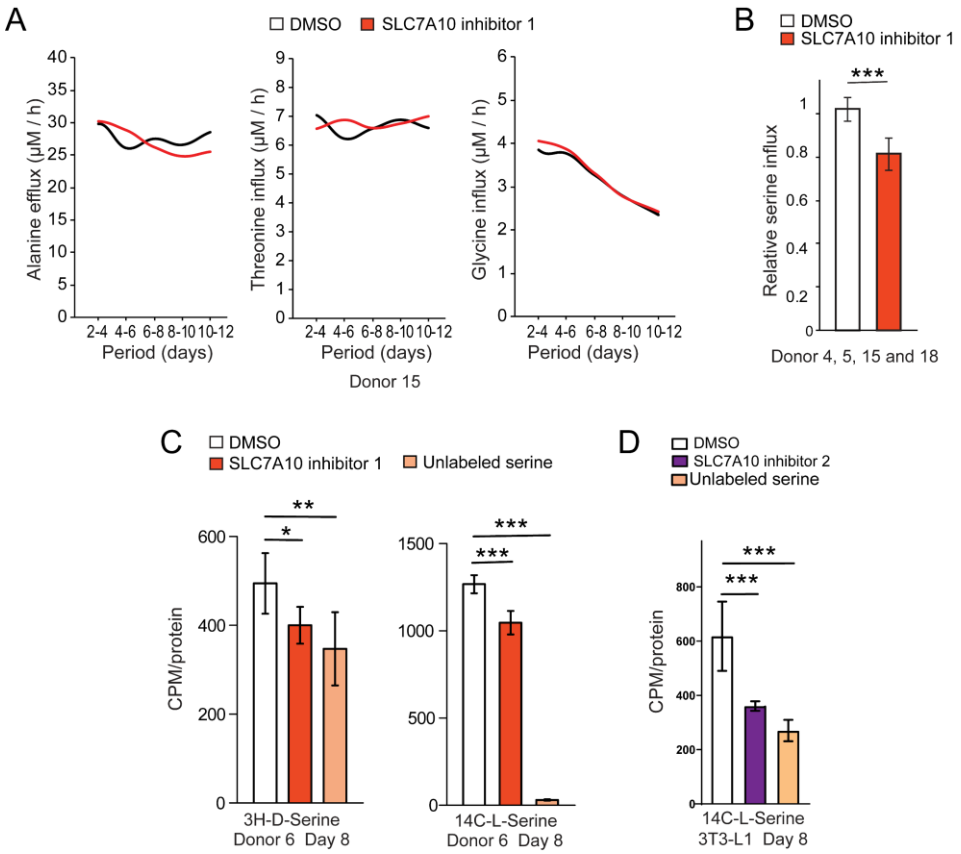

Supplementary Figure 7. Inhibition of SLC7A10 in human primary and mouse adipocytes regulates adipocyte serine uptake and redox status.

(**A**) Changes in alanine, threonine and glycine flux was not alter for hASCs treated with SLC7A10 inhibitor 1 throughout differentiation. Amino acid flux was calculated based on the amino acid concentrations in unconditioned medium and change in concentrations upon cell culture during 48-hour periods. Data for two replicate wells for a representative experiment are shown.

(**B**) The average reduction in serine influx due to SLC7A10 inhibition was calculated (as in A) for fully differentiated hASCs (day 10-12), for replicate experiments in cells from four different people.

(**C**) hASCs were treated with SLC7A10 inhibitor 1 for 30 minutes at day 8 of differentiation. Thereafter, radiolabeled 3H-D-serine (1 µM) or 14C-L-serine (1 µM) was added for 30 minutes and cellular uptake of the radiolabeled amino acids was measured in cell lysate. Unlabeled D-serine and L-serine (100 mM) were used as positive control of uptake inhibition. Data are presented as mean ± SD (n=3-6).

(**D**) 3T3-L1s were treated with SLC7A10 inhibitor 2 for 30 minutes at day 8 of differentiation. Thereafter, radiolabeled 14C-L-serine (1 µM) was added for 30 minutes and cellular uptake of the radiolabeled amino acids was measured in cell lysate. Unlabeled L-serine (100 mM) were used as positive control of uptake inhibition. Data are presented as mean ± SD (n=6).

*, $p<0.05$, **, $p<0.01$. ***, $p<0.001$.

Supplementary References

1. Mi H, Muruganujan A, Huang X, Ebert D, Mills C, Guo X, et al. Protocol Update for large-scale genome and gene function analysis with the PANTHER classification system (v.14.0). Nat Protoc [Internet]. 2019 Mar 25 [cited 2019 Apr 4];14(3):703–21. Available from: http://www.nature.com/articles/s41596-019-0128-8
2. Eden E, Navon R, Steinfeld I, Lipson D, Yakhini Z. GOrilla: a tool for discovery and visualization of enriched GO terms in ranked gene lists. BMC Bioinformatics [Internet]. 2009 Feb 3 [cited 2018 Jan 31];10(1):48. Available from: http://www.ncbi.nlm.nih.gov/pubmed/19192299
3. Supek F, Bošnjak M, Škunca N, Šmuc T. REVIGO Summarizes and Visualizes Long Lists of Gene Ontology Terms. Gibas C, editor. PLoS One [Internet]. 2011 Jul 18 [cited 2019 Mar 27];6(7):e21800. Available from: https://dx.plos.org/10.1371/journal.pone.0021800